

Investigation of the stability and charge states of vacancy in clusters Si_{29} and Si_{38}

A. B. Normurodov *, A. P. Mukhtarov , F. T. Umarova , M. Yu. Tashmetov ,
Sh. Makhkamov , N. T. Sulaymonov 

Institute of nuclear physics, 1 Xuroson Str., 100214, Tashkent, Uzbekistan

Received May 08, 2021, in final form December 07, 2021

Stability and charge states of vacancy in Si_{29} and Si_{38} clusters have been calculated by non-conventional tight-binding method and molecular dynamics. Based on the theoretical calculations, it was shown that the vacancy in pure dimerized clusters is unstable, while in hydrogenated $\text{Si}_{29}\text{H}_{24}$ and $\text{Si}_{38}\text{H}_{30}$ clusters it is stable, but leads to a distortion of its central part with the transition of symmetry from Td to C_{3v} and a change in the forbidden gap. The charges of cluster atoms in the presence of a vacancy are distributed so that all silicon atoms acquire a stable negative charge, which occurs due to the outflow of electrons of the central atom to the neighboring spheres.

Key words: *silicon nanoclusters, charge, vacancy, non-conventional tight-binding method, molecular dynamics*

1. Introduction

Silicon nanoparticles as well as crystalline silicon may contain various defects that effect both their optoelectronic and electrophysical properties. The most common defects are the point defects caused by an intrinsic interstitial atom and a vacancy. Moreover, a vacancy can be formed both inside and on the surface of nanoparticles during the crystal growth and under various external influences. The vacancy in crystalline silicon Si was studied in detail. For example, the stable states of the vacancy and its complexes with impurities, their formation energies were theoretically investigated in previous researches [1–5]. The experimental studies [6–10] indicated the possibility of forming the complexes of a vacancy with an impurity oxygen and hydrogen atoms in stable states, and the kinetic energies of the formation are given. This type of defects are very mobile and could be identified directly only in the silicon of *p*-type. The vacancy in bulk Si known to form highly localized defect complexes with deep local levels in the band gap of silicon [10]. The possibility of preserving the energy characteristics of such a defect complex in nanosized particles and the effect of size-dependent phenomena of a particle have not been unambiguously determined.

Controlling the concentration of the vacancy in silicon is one of the key factors in semiconductor electronics. Despite the fact that the vacancy in crystalline silicon has been studied for a long time using various methods, a relatively little attention is paid to the presence and stability of the vacancy in silicon nanoparticles. Although a number of researches on vacancy in nanosilicon have been provided [11–14], detailed studies of its geometric configuration and positions of electronic levels were done only in several of them [13, 15]. Thus, size effects on the vacancy formation energy and entropy were considered in [13] and it was found that the size reduction makes the vacancy much easier to form; then, the vacancy concentration increases with reducing size and increasing temperature.

Thermodynamic state equation of the nanocrystal with vacancies leads to the conclusion that, regardless of the presence of an external effect on the nanoparticle, even at a constant total temperature

*Corresponding author: normurodov@inp.uz, anormurodov@gmail.com.

of the system of interacting atoms, a certain number of vacancies always formed due to thermal fluctuations [15]. Therefore, the determination of the structure of the local region of the defect formation with the participation of a vacancy and the effect of the surface on the stability of the defect is of great importance. Zhang *et al.* researched the quantum confinement effect on the vacancy-induced spin polarization in carbon, silicon, and germanium nanoparticles by density functional analysis [16, 17].

This paper presents the results of studies of the structural parameters and energy characteristics of pure and hydrogenated silicon nanoparticles Si_{29} and Si_{38} with vacancies. Such sized clusters are most stable and widely used models of the silicon nanoparticle of one nm size [18, 19]. At present, the computational capabilities make it possible to calculate the main structural and energy parameters of such clusters by *ab initio* methods. However, there are two very important disadvantages of both groups of Hartree–Fock–Rutaan methods and the methods based on the density functional theory. Taking account of the real conditions for the existence of nanoparticles first of all leads to spending a huge computer time for calculations while a large overestimation of the internal bonds total energy makes it difficult to compare the calculated energy parameters with experimental data. For the above reasons, we decided to apply the non-conventional tight-binding method (NTBM) [20] to the calculations, which with a correct approach to the parameterization procedure and the choice of the calculation algorithm, makes it possible to achieve a significant reduction in computational costs and a reasonable agreement with experimental data.

2. Computation method details

The method for simulation of nanostructures used by us is adapted to optimize the structure and energy parameters and combines the NTBM proposed by Khakimov [20, 21], and the molecular dynamic method. Here, the expression for the total energy of the NTBM has the form

$$E_{\text{tot}} = \sum_{\mu} \sum_{\nu > \mu} \frac{Z_{\mu}^{\text{scr}} Z_{\nu}^{\text{scr}}}{R_{\mu\nu}} + \sum_{\mu} \sum_{\nu > \mu} \frac{Q_{\mu} Q_{\nu}}{R_{\mu\nu}} + \sum_{\mu} \sum_{\nu > \mu} \sum_i \sum_j P_{\mu i, \nu j} H_{\mu i, \nu j} + \sum_{\mu} (E_{\mu} - E_{\mu}^0), \quad (2.1)$$

where $R_{\mu\nu}$ is internuclear distance,

$$Z_{\mu}^{\text{scr}} = Z_{\mu}^{\text{scr}}(R_{\mu\nu}, \{N_{\mu i}^0\}) = Z_{\mu} - \sum_i N_{\mu i}^0 \left[1 - \alpha_{\mu i} \exp\left(-\alpha_{\mu i} R_{\mu\nu} / R_{\mu}^0\right) \right], \quad (2.2)$$

$$Q_{\mu} = Z_{\mu}^{\text{scr}}(R_{\mu\nu}, \{N_{\mu i}^0\}) - Z_{\mu}^{\text{scr}}(R_{\mu\nu}, \{N_{\mu i}^0\}) - Z_{\mu}^{\text{scr}}(R_{\mu\nu}, \{N_{\mu i}\}) \quad (2.3)$$

are screened nuclear and non-point ion charges, respectively; Z_{μ} is the charge of the μ -th nucleus or the nucleus with core electrons; $R_{\mu}^0 = n / \xi_{\mu}^0$ is the most probable distance between the nucleus and electron, n and ξ_{μ}^0 is the principal quantum number and Slater exponent of the i -th atom orbital (AO), centered on μ -nucleus; E_{μ}^0 and E_{μ} are total energies of the individual atoms in non-interacting and interacting systems, characterized by $\{N_{\mu i}^0 \equiv P_{\mu i, \mu i}^0\}$ and $\{N_{\mu i} \equiv P_{\mu i, \mu i}\}$ occupancy numbers and $\{E_{\mu i}^0\}$ and $\{E_{\mu i}\}$ corresponding valence AO's energies. AO is supposed to be orthogonalized, and the matrix equation will be as follows:

$$\sum_{\nu j} (H_{\mu i, \mu j} - \epsilon \delta_{\mu i, \nu j}) C_{\nu j} = 0, \quad (2.4)$$

and used to be solved self-consistently for determination of the ϵ_k energetic spectra and $C_{\mu j}$ expansion coefficients of the molecular orbitals (MO) over AO. Self-consistent calculations are based on iterative recalculation of the diagonal matrix elements of the Hamiltonian using the dependency of the bond order matrix

$$P_{\mu i, \nu j} = \sum_k N_k C_{\mu i}(k) C_{\nu j}(k), \quad (2.5)$$

and $N_{\mu i} \equiv P_{(\mu i, \mu i)}$ AO occupancy from $C_{\nu j}$. Here, k denotes a MO and N_k — denotes the occupancy number of the k -th MO. In conventional tight-binding method (TBM), the N_k are all equal to 2 (except the highest MO of a system with an odd number of electrons). However, NTBM involves a description of charged and excited systems, where one or more MOs may have an occupancy less than 2.

The diagonal and off-diagonal matrix elements of NTBM have the form

$$P_{\mu i, \mu j} = \left(E_{\mu i} - \sum_{\nu \neq \mu} Q_{\nu} / R_{\mu \nu} \right) \delta_{ij}, \quad (2.6)$$

and

$$H_{\mu i, \nu j} = \pm \frac{1}{2} h_{\mu i} h_{\nu j} A_{ij}(\vec{R}_{\mu \nu}), \quad \nu \neq \mu, \quad (2.7)$$

correspondently

$$h_{\mu i} = b_{\mu i} \xi_{\mu i}^0 \exp \left(-\beta_{\mu i} R_{\mu \nu} / \bar{R}_{\mu i}^0 \right) F_{\mu i}, \quad (2.8)$$

$$F_{\mu i} = \left\{ 1 + \exp \left[-\gamma_{\mu i} (R_{\mu \nu} - d_{\mu i}) \right] \right\}^{-1}, \quad (2.9)$$

$\bar{R}_{\mu i}^0$ is the average distance between electron and corresponding nucleus, $A_{ij}(\vec{R}_{\mu \nu})$ are angular functions tabulated by Slater and Coster [21]. In (2.7), plus sign is taken for sp and $pp - \sigma$ matrix elements, and minus sign is taken for ss and $pp - \pi$ matrix elements.

NTBM yields to traditional TBM in speed due to iterative self-consistent calculations. To accelerate the convergence of these calculations, we use the techniques of dynamic damping [20] and shift level [22]. A more rigorous criterion for self-consistency was used to calculate clusters; the calculations at each point in configuration-coordinate space are completed only if the values of AO population in two successive iterations are less than 10^9 .

To determine the possible spatial structures of the system of a given number of atoms, the molecular dynamics simulation (MD) method [23, 24] based on numerical integration of Newton's equations of motion was used:

$$m_i d^2 r_i / dt^2 = m_i a_i = F_i; \quad F_i = -dU/dr_i, \quad (2.10)$$

where m_i , r_i and a_i are, accordingly, the mass, position and acceleration of the i -th particle; F_i is force acting to the i -th particle by other particles; U is total potential energy of the system, which can be calculated using one of the approximate methods.

Equation (2.10) can be solved by step using Taylor expansion near current t time [22]:

$$r_{t+\delta t} = r_t + v_t \delta t + \frac{1}{2} a_t \delta t^2 + \frac{1}{6} b_t \delta t^3 + \dots, \quad (2.11)$$

$$v_{t+\delta t} = v_t + a_t \delta t + \frac{1}{2} b_t \delta t^2 + \frac{1}{6} c_t \delta t^3 + \dots, \quad (2.12)$$

where v is velocity of the particle.

To integrate the equation of motion, a third-order algorithm is used in which the positions R and particle velocities v are calculated by the following formulas:

$$R_{t+\delta t} = \left[R_t + v_t \delta t + \frac{1}{12} (7a_t - a_{t-\delta t}) \delta t^2 \right] \cdot \left(\frac{1}{12} \frac{da_t}{dR_t} \delta t^2 \right)^{-1}, \quad (2.13)$$

$$v_{t+\delta t} = v_t + \frac{1}{12} (8a_t + 5a_{t+\delta t} - a_{t-\delta t}) \delta t, \quad (2.14)$$

where a_t is acceleration of the particle with m mass at t time moment, da_t/dR_t is a derivative from acceleration over coordinates of the R particle. In calculating the forces (accelerations) numerically, their derivatives can be determined simultaneously using the same two additional calculated values of the total energy in the positions $R_t + \delta R$ and $R_t - \delta R$ (δR is small shift):

$$a_t = -\frac{1}{m} \frac{E(R_t + \delta R) - E(R_t - \delta R)}{2\delta R}, \quad (2.15)$$

$$\frac{da_t}{dt} = -\frac{1}{m} \frac{E(R_t + \delta R) + E(R_t - \delta R) - 2E(R_t)}{\delta R^2}. \quad (2.16)$$

A self-consistent calculation of the electron density distribution is made many times for each nuclear configuration of the system, starting with a trial set of values $\{N_{\mu i}\}$, while the difference between the input and output values $\{N_{\mu i}\}$ (or $\{c_i\}$) in solving secular equation 2.13 gets negligible:

$$\sum_{\mu i} \sum_{\nu j} (H_{\mu i, \nu j} - \epsilon \delta_{ij} \delta_{\mu\nu}) c_{\nu j} = 0, \quad (2.17)$$

where $\{\epsilon_k\}$ are electronic energetic levels, $c_{\nu j}$ are expansion coefficients of wave functions for AO, i and j are atomic orbitals, H is Hamiltonian of the atomic system, δ are average quadratic errors.

3. Results and discussions

This work presents the results of studying the stability of a vacancy both in pure Si_{29}D and Si_{38}D clusters and in their hydrogenated samples. As a model of a nanoparticle we have chosen a silicon nanocluster Si_{29}D with a dimerized surface and saturation of the surface 24 silicon atoms with hydrogen atoms. This cluster is atomically centered and the symmetry of the central atom is tetrahedral. While considering the vacancy, the central atom was removed from the cluster and later the cluster geometry was optimized.

The obtained results show (figure 1) that a vacancy in a pure Si_{29}D cluster is unstable and undergoes a collapse as a result of a shift of cluster atoms. In this case, the disorder of the cluster structure increases. Only in the case of a positively charged Si_{29}D cluster the presence of a vacancy in the center leads to the formation of a hollow Si_{29} cluster with a diameter of 7.04 Å.

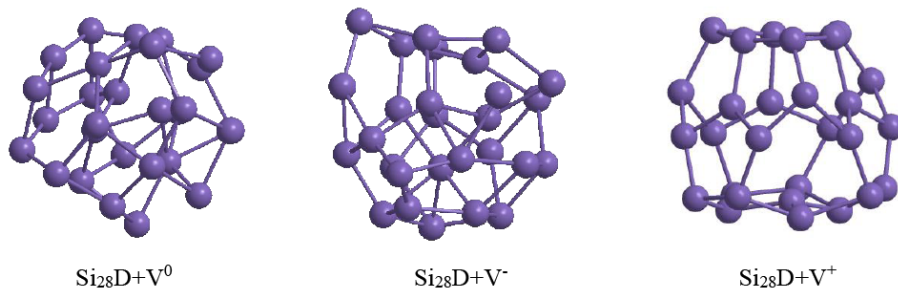


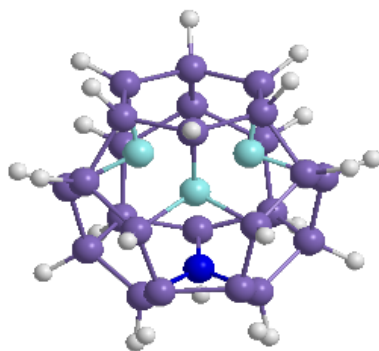
Figure 1. (Colour online) Surface dimerized and optimized cluster structures with vacancy in different charge states.

The obtained dependences of the densities of vacancy energy states in a dimerized Si_{29}D (table 1) show that the density of vacancy states in the neutral dimerized Si_{29}D coincides with the density of states for the pure dimerized Si_{29}D without a vacancy and indicate the metallic nature of conductivity (table 1). The HOMO–LUMO gap in these clusters is of the order of 0.01 eV. In the charged clusters the gap grows. Investigation of the stability of a neutral vacancy in a surface-dimerized $\text{Si}_{29}\text{DH}_{24}$ cluster with passivation of unsaturated bonds has showed that four silicon atoms, the first neighbors of the vacancy, initially had

Table 1. The calculated characteristics of the surface dimerized pure silicon cluster with a vacancy in different charge.

Clusters	Atomization energy, eV	Atomization energy per atom, eV	Bond length, Å	HOMO–LUMO gap, eV
Si ₂₉ D	124.33	4.28	2.29	0.08
Si ₂₈ + V ⁰	120.51	4.30	2.39	0.09
Si ₂₈ + V ⁻	120.58	4.29	2.38	0.15
Si ₂₈ + V ⁺	117.75	4.20	2.35	0.26

a symmetrical arrangement corresponding to the tetrahedral point symmetry group. They underwent a Jahn–Teller type distortion from the initial positions. Three atoms as shown in figure 2 approach each other while one of the Si atoms moves away towards the surface. As a result, the nearest hydrogen atom connected to the surface atom shifts to a bonded-centered position in the direction of the remote silicon atom. The symmetry of the central part of the cluster transfers from the symmetry point group T_d to the symmetry point group C_{3v} (lowering of the T_d symmetry upon transition to the hexagonal position). In this case, the distance between the three atoms becomes 3.19 Å (ideally 3.75 Å). It increases 4.12 Å for the removed atom and one of the three connivent atoms. The second neighbors of the vacancy also move away and the distances between the first and second neighbors of the vacancy become 2.28 Å.

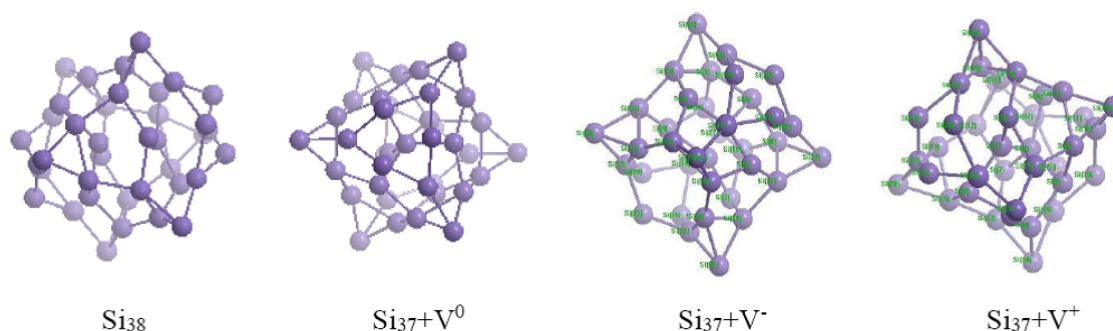
**Figure 2.** (Colour online) The structure of the vacancy in the dimerized Si₂₉H₂₄ cluster. Silicon atoms are the first neighbors of a vacancy and are shown in a color different from the surrounding Si atoms (the blue atoms are the atoms shifted to each other, the dark blue is a distant atom).

The charges of cluster atoms in the presence of a vacancy are distributed so that all silicon atoms acquire a stable negative charge that occurs due to the outflow of the electrons of the central atom to the neighboring spheres. This can be seen from table 2 where the values of the charges in the two coordination spheres of the cluster change to a great extent. In the third sphere, the charge changes are insignificant compared to the cluster without a vacancy. The presence of a vacancy leads to a substantial rearrangement of the bonds among the nearest neighbors of the vacancy and gives a number of energy levels in the gap between the HOMO and LUMO. Apparently, this is due to the approach of the three atoms and the formation of a weak covalent bonds between them. At the same time, the fourth atom tends to float to the surface at an equal distance from the center of the cluster. To determine the effect of a vacancy for the structural rearrangement of the Si₃₈ cluster, the equilibrium geometries and the energy parameters of a number of clusters were calculated. We have investigated those for dimerized Si₃₈ cluster without a vacancy, three charge states (0, +, -) of the Si₃₇ cluster with a vacancy in the center formed from the Si₃₈ cluster by the removal of one of the central atoms. MD optimized structures of the pure Si₃₈ cluster and with a vacancy in the center in different charge states are shown in figure 3. Table 3 shows the atomization energies and the HOMO–LUMO gap. As can be seen from figure 3, the cluster structure during the formation of a vacancy retains a tetrahedral symmetry of the cubic system. However, the volume of the central part of clusters with a vacancy decreases because of an increase in the length of

Table 2. The calculated parameters in the hydrogenated cluster $\text{Si}_{29}\text{H}_{24}$ and in the presence of a vacancy.

Clusters	Total energy, eV	HOMO–LUMO energy gap, eV	First Neighbor Shift	Charges				
				Central atom	1 sphere	2 sphere	3 sphere	Hydrogen atoms
$\text{Si}_{29}\text{H}_{24}$	181.39	1.02		0.20	–0.13	–0.14	0.01	0.05
$\text{Si}_{28}\text{H}_{24}\text{V}$	173.48	0.09	C_{3v} $3x(-0, 56)$ $1x(+0, 37)$	–	–0.08	–0.08	–0.04	0.05

Si-Si bonds between atoms. The number of possible configurations of these clusters containing a vacancy in the center is equal to the number of hexagonal positions around the tetrahedral center, i.e., equal to 6. With the removal of one silicon atom from the Si_{38} cluster, the atomization energy slightly decreases, and the most stable is a negatively charged cluster with a vacancy in the center. The HOMO–LUMO gap increases by a factor of 2 for $\text{Si}_{37} + V^0$, and decreases by a factor of 2 for $\text{Si}_{37} + V^+$. The analysis of the components of the atomization energy (table 4) shows that, in the presence of a vacancy, the contribution of the ion-ion interaction sharply increases for a positively charged state.

**Figure 3.** (Colour online) Optimized bare and vacancy-consisted Si_{38} cluster structures.**Table 3.** The calculated characteristics of vacancy-consisted Si_{38}D cluster in different charge states.

Clusters	Si-Si bond length, Å	Atomization energy per atom, eV	HOMO–LUMO gap, eV
Si_{38}D	2.28	4.25	0.15
$\text{Si}_{37} + V^0$	2.35	4.16	0.30
$\text{Si}_{37} + V^-$	2.33	4.17	0.22
$\text{Si}_{37} + V^+$	2.36	4.14	0.08

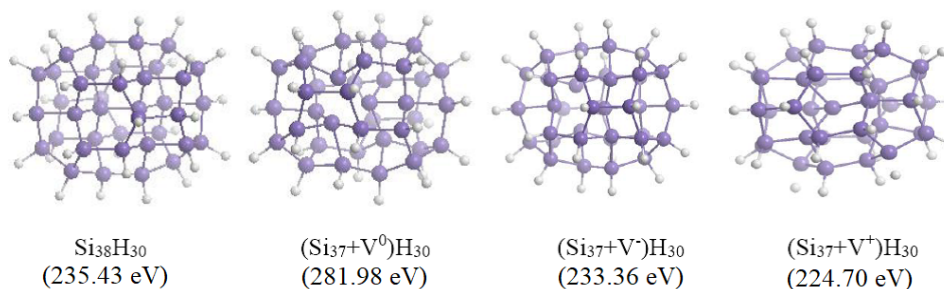
Accordingly, the bond between the atoms of the cluster core and surface atoms is weakened. Since in all cases the positive charge of the cluster surface is preserved, it can be assumed that this occurs due to a change in the electron densities inside the clusters.

The study of hydrogen passivated clusters in the presence of a vacancy shows that complete hydrogen passivation of dangling bonds on the surface stabilizes (freezes) the structure of clusters with the surface reconstruction. Figure 4 comparatively shows the structure and atomization energies of the studied

Table 4. Components of atomization energy of clusters consisting of 38 atoms with a vacancy in different charge states.

Dimerized cluster	Atomization energy, eV	Atom-atom interaction, eV	Binding energy, eV	Ion-ion interaction, eV
Si ₃₈	161.39	48.24	286.54	0.90
Si ₃₈ ⁻	165.31	48.54	287.19	0.91
Si ₃₈ ⁺	154.77	47.99	286.43	2.99
Si ₃₇ + V ⁰	154.13	47.21	280.56	0.77
Si ₃₇ + V ⁻	154.22	46.08	277.15	0.31
Si ₃₇ + V ⁺	153.22	44.03	273.06	2.90

clusters. As can be seen from figure 4, the presence of a vacancy distorts the cluster structure while maintaining the tetrahedral symmetry of the bonds. A neutral, passivated by hydrogen, Si₃₈ cluster containing a vacancy is more stable than a cluster without a vacancy, the difference being 46.55 eV. In the case of the (Si₃₇ + V⁺)H₃₀ cation, the cluster volume increased by about 10%, and the central atom shifted toward the vacancy with the formation of a bond with the peripheral silicon atom. The values of

**Figure 4.** (Colour online) Geometry of optimized Si₃₈ clusters in different charge states with complete passivation of surface bonds.

atomization energies are given in parentheses. Table 5 shows the atomization energy and the HOMO–LUMO gap for passivated clusters. As can be seen, in general, the passivation of hydrogen by clusters containing a vacancy does not change the atomization energy with the exception of (Si₃₇ + V⁰)H₃₀, but the gap significantly decreases compared to a cluster without a vacancy. Among the clusters containing a

Table 5. Atomization energies and gap widths of hydrogen-passivated and vacancy-consisted clusters in different charge states.

Clusters	Atomization energy per atom, eV	HOMO–LUMO gap, eV
Si ₃₈ H ₃₀	3.46	0.92
(Si ₃₇ + V ⁰)H ₃₀	4.21	0.18
(Si ₃₇ + V ⁻)H ₃₀	3.46	0.24
(Si ₃₇ + V ⁺)H ₃₀	3.47	0.17

vacancy, the largest HOMO–LUMO gap is observed in a negatively charged cluster. Thus, in the presence of a vacancy, the cluster structure is distorted, and the electronic properties change.

Conclusions

Thus, based on the theoretical calculations, it was shown that the vacancy in pure dimerized clusters is unstable, while in hydrogenated $\text{Si}_{29}\text{H}_{24}$ and $\text{Si}_{38}\text{H}_{30}$ clusters it is stable, but it leads to a distortion of its central part with the transition of symmetry from T_d to C_{3v} and a change in the forbidden gap. The presence of a vacancy leads to a substantial rearrangement of the bonds between the nearest neighbors of the vacancy and gives a number of energy levels to the gap region between the HOMO and LUMO. Apparently, this is due to the approach of the three atoms and the formation of a weak covalent bond between them, while the fourth atom appears to float to the surface at the same distance from the center of the cluster. The charges of cluster atoms in the presence of a vacancy are distributed so that all silicon atoms acquire a stable negative charge, which occurs due to the outflow of electrons of the central atom to the neighboring spheres.

References

1. Marqués L. F., Pelaz L., Hernández J., Barbolla J., Gilmer G. H., Phys. Rev. B, 2001, **64**, 045214, doi:10.1103/PhysRevB.64.045214.
2. Dabrowski J., Kissinger G., Phys. Rev. B, 2015, **92**, 144104, doi:10.1103/PhysRevB.92.144104.
3. Hwang G. S., Goddard W. A., Phys. Rev. B, 2002, **65**, 233205, doi:10.1103/PhysRevB.65.233205.
4. Lee Y., Lee S., Hwang G. S., Phys. Rev. B, 2011, **83**, 125202, doi:10.1103/PhysRevB.83.125202.
5. Prasad M., Sinno T., Appl. Phys. Lett., 2002, **80**, 1951, doi:10.1063/1.1461050.
6. Johannesen P., Nielsen B. B., Byberg J. R., Phys. Rev. B, 2000, **61**, 4659, doi:10.1103/PhysRevB.61.4659.
7. Kolevator I. L., Weiser P. M., Monakhov E. V., Svensson G. B., Phys. Status Solidi A, 2018, **216**, 1800670, doi:10.1002/pssa.201800670.
8. Watkins G. D., Radiation Damage in Semiconductors, Royaumont, Paris, 1964.
9. Platonenko A., Colasuonno F., Gentile F. S., Pascale F., Dovesi R., J. Chem. Phys., 2021, **154**, 174707, doi:10.1063/5.0044106.
10. Emtcev V. V., Mashovetv E. V., Impurities and Point Defects in Semiconductors, Radio i Sviaz, Moscow, 1981, (in Russian).
11. Magomedov M. N., J. Surf. Invest., 2018, **12**, 185–196, doi:10.1134/S1027451018010299.
12. Zhu X., Wang Z., Int. J. Nanotechnol., 2006, **3**, No. 4, 492–516, doi:10.1504/IJNT.2006.011175.
13. Guisbiers G., J. Phys. Chem. C, 2011, **115**, No. 6, 2616–2621, doi:10.1021/jp108041q.
14. Barcaro G., Carravetta V., Sementa L., Monti S., Adv. Phys.: X, 2019, **4**, No. 1, 1–18, doi:10.1080/23746149.2019.1634487.
15. Chernyshev A. P., In: 11th International Forum on Strategic Technology (IFOST), IEEE, Novosibirsk, 2016, doi:10.1109/IFOST.2016.7884136.
16. Zhang Z., Dai Y., Huang B., Whangbo M. H., Appl. Phys. Lett., 2010, **96**, 062505, doi:10.1063/1.3302463.
17. Khrantsov I. A., Fedyanin D. Yu., Nanomaterials, 2020, **10**, 361, doi:10.3390/nano10020361.
18. Tereshchuk P. L., Khakimov Z. M., Umarova F. T., Swihart M. T., Phys. Rev. B, 2007, **76**, 125418, doi:10.1103/PhysRevB.76.125418.
19. Ossicini S., Bisi O., Degoli E., Marri I., Iori F., Luppi E., Magri R., Poli R., Cantele G., Ninno D., Trani F., Marsili M., Pulci O., Olevano V., Gatti M., Gaal-Nagy K., Incze A., Onida G., J. Nanosci. Nanotechnol., 2008, **8**, 479–492, doi:10.1166/jnn.2008.A009.
20. Khakimov Z. M., Comput. Mater. Sci., 1994, **3**, 95–108, doi:10.1016/0927-0256(94)90156-2.
21. Khakimov Z. M., Tereshchuk P. L., Sulaymanov N. T., Umarova F. T., Swihart M. T., Phys. Rev. B, 2005, **72**, 115335, doi:10.1103/PhysRevB.72.115335.
22. Slater J. C., Koster C. F., Phys. Rev., 1954, **94**, 1498, doi:10.1103/PhysRev.94.1498.
23. Allen M. P., Tildesley D. J., Computer Simulation of Liquids, Clarendon Press, Oxford, 1987.
24. Wolkin M. V., Jorne J., Fauchet P. M., Allan G., Delerue C., Phys. Rev. Lett., 1999, **82**, No. 1, 197, doi:10.1103/PhysRevLett.82.197.

Дослідження стійкості і зарядових станів вакансії в кластерах Si₂₉ і Si₃₈

А. Б. Нормуродов , А. П. Мухтаров , Ф. Т. Умарова , М. Ю. Ташметов ,
Ш. Махкамов , Н. Т. Сулеймонов 

Інститут ядерної фізики, вул. Хуросонська 1, 100214, Ташкент, Узбекистан

За допомогою нестандартного методу сильного зв'язку та молекулярної динаміки розраховані стійкість і зарядові стани вакансії в кластерах Si₂₉ і Si₃₈. На основі теоретичних розрахунків було показано, що вакансія в чистих димеризованих кластерах є нестійкою, в той час як в гідрогенізованих Si₂₉H₂₄ та Si₃₈H₃₀ кластерах вона є стійкою, але призводить до деформації центральної частини кластерів зі зміною симетрії з Td до C_{3v} та до змін в забороненій зоні. Заряди атомів кластера при наявності вакансії розподілені таким чином, що всі атоми кремнію набувають стійкого від'ємного заряду, що відбувається завдяки відтоку електронів центрального атома на сусідні сфери.

Ключові слова: нанокластери кремнію, заряд, вакансія, нестандартний метод сильного зв'язку, молекулярна динаміка
